Integrating Tactile and Force Feedback with Finite Element Models

Christopher R. Wagner, Douglas P. Perrin,
Ross L. Feller, and Robert D. Howe
Division of Engineering and Applied Sciences
Harvard University, Cambridge, MA, USA
{*cwagner,rfeller,dperrin,howe*}*@deas.harvard.edu*

Olivier Clatz, Hervé Delingette, and Nicholas Ayache
EPIDAURE, INRIA Sophia-Antipolis
BP 93, F-06902 Sophia Antipolis Cedex, France
{*Olivier.Clatz, Herve.Delingette, Nicholas.Ayache*}*@sophia.inria.fr*

Abstract— **Integration of the correct tactile and kinesthetic force feedback response with an accurate computational model of a compliant environment is a formidable challenge. We examine several design issues that arise in the construction of a compliance renderer, specifically the interaction between impedances of tactile displays, impedances of robot arms, and the computational model. We also describe an implementation of a compliance rendering system combining a low-impedance robot arm for large workspace kinesthetic force feedback, a high-impedance shape display for distributed tactile feedback to the finger pad, and a real-time finite element modeler. To determine the efficacy of the integration of tactile and kinesthetic force feedback components, we conducted a study examining the user's ability to discriminate stiffness. Subjects were able to reliably detect a 20% difference in rendered material stiffness using our compliance rendering system.**

I. Introduction

Haptic feedback promises to greatly enhance the capabilities of virtual environment systems. This is particularly important in medical training systems, where many tasks require precise manipulation and perception skills. These tasks often involve contact between the finger tip and soft tissue. A central example is palpation, where physicians and surgeons use their sense of touch to feel a pulse, locate hidden structures, or determine the mechanical properties of tissue. Lederman and Klatzky [1] have shown that if distributed tactile sensations across the finger tip are absent, many sensory and perceptual capabilities are greatly impaired. Therefore, the computational model of the finger-tissue interaction must generate both kinesthetic (e.g. force) and tactile feedback and the hardware must display both feedback modalities.

With few exceptions, haptic feedback from current systems involving soft tissue interactions have used only kinesthetic feedback. Most work has concerned minimally invasive surgery trainers (e.g. [2], [3]), where the soft tissue interacts with rigid surgical instruments. In this situation, distributed skin sensations need not be portrayed. A focus of this research area has been the development of real-time mechanical models for the tissue-instrument interaction, with varying degrees of realism; these models may be immediately useful in applications that require tactile feedback signals as well. Similarly, work on the use of tactile displays for palpation training [4] [5] [6] have not included kinesthetic feedback and have used only rudimentary models for the finger-tissue mechanical interaction.

In this paper we consider the design of a virtual reality system that provides both kinesthetic and tactile feedback based on a mechanics-based model of the interaction between the finger tip and a complaint object. A key issue in the development of such a system is the selection of compatible hardware and model configurations, particularly with respect to the devices' mechanical impedances and the mechanical model boundary conditions. We begin with an analysis of the various potential components of these systems and define compatibility constraints. Next, we implement one version of the system using a high-impedance tactile shape display mounted on a low-impedance robot arm, used here as a force feedback device. A real-time FEM model accepts user-imposed motion of the device as the input boundary condition and generates force and tactile shape feedback commands. Finally, to confirm the functionality of the system, we conduct a simple user study that compares material stiffness perception with force and tactile feedback versus force feedback alone. The results demonstrates that the tactile display adds to perceptual capabilities in simulated soft tissue interactions.

II. Design Issues

Haptic portrayal of compliant surfaces requires a hardware display system and a computational model of the mechanics of finger-tissue interaction. For best accuracy, the computational model needs to simulate the interaction between the compliant human finger and the compliant material, calculating the appropriate tactile and kinesthetic feedback that result from user input of motions or forces. The haptic display hardware then needs to faithfully reproduce the desired force or shape output from the computational model. We examine several design issues that follow from integrating the computational model with the haptic display system.

A. Computational model

To understand the functional requirements of the computational model, it is instructive to examine the behavior of the human finger tip as it is pressed into a compliant object [7] [5]. As seen in Fig. 1, the finger undergoes both a net displacement into the object and a deformation of the
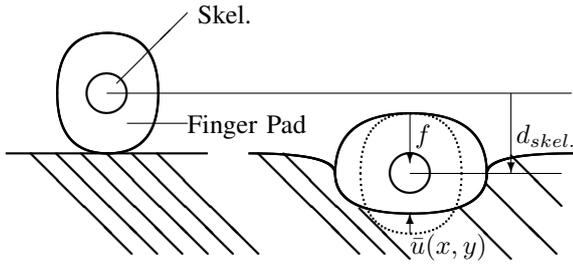
Fig. 1. Cross section though finger and compliant slab of material. Left: prior to application of contact force; Right: finger indenting material

finger pad. The nature of this deformation depends on the geometry, mechanical properties, and contact conditions of the finger and the complaint object.

For the purposes of haptic display, it is easiest to specify this interaction in terms of the displacement and force at the bone at the center of the finger, as mechanical interactions with the display system are largely transmitted to the user's musculoskeletal system through the bones. The input boundary conditions for the model may then be either the force f_{skel} or displacement d_{skel} applied by the user to the finger tip (Fig. 2). The selection of either f_{skel} or d_{skel} as the input is determined by impedance characteristics of the haptic display devices, as detailed below. The model then calculates the complementary variable d_{skel} or f_{skel}, as well as the surface deformation $\bar{u}(x,y)$ and the surface stress tensor $\bar{\sigma}(x,Y)$ of the finger tip skin along the contact surface (x,y) with the object. These signals then drive the haptic display devices.

In general, these are demanding mechanical calculations. Measurements of the mechanical properties of the human finger pad under typical manipulation forces show large nonlinearities [8] [9], due to both material constitutive properties and large deformations. In addition, the contact area with the compliant material will change as a function of the contact force. Commercial FEM packages designed to optimize accuracy for mechanical design applications take many hours to solve a single indentation case, and often fail to converge with realistic material properties and loading states.

As determined in surgical simulation research, a number of shortcuts can trade off speed for accuracy. A straightforward example is the use of linear material properties for both the finger and the complaint object. Another step is the use of a simple model to represent the finger-object contact. One such model is the use of a fixed diameter pressure distribution to represent the surface stress tensor of the finger tip. For a given overall force, the stress tensor $\bar{\sigma}(x,Y)$ is given by the scaled pressure distribution and the resulting surface deformation $\bar{u}(x,y)$ is calculated from the FEM model. A similar simplification can be made if the input is a position: the surface deformation $\bar{u}(x,y)$ is given by a scaled displacement distribution and the resulting stress tensor and contact force is computed in the FEM model. When using a simplified model it is necessary

to match the inputs and outputs of the model with the impedance requirements of the haptic devices, as discussed below.

There are also several options for the mechanical calculation engine. One approach is to precompute a sample of all possible user inputs (forces/moments or positions/orientations), which can yield highly accurate, potentially nonlinear models through the use of commercial FEM packages. The resulting lookup table becomes unreasonably large with a large range of multidimensional user inputs, as will be the case for complex environments. This limits the ability to perform the vast number of required precomputations or index and interpolate within the table in real-time.

"Real time" FEM is useful for rendering reasonably sized meshes, especially when the number of potential user input values are large and when the mesh changes form throughout the simulation, as in surgical simulation with cutting [3]. This speed comes with a trade off in accuracy, however, as calculations are assumed linear to reduce the computation time. Hybrid approaches exist, such as interpolating/switching between linear models at different force/indentation ranges. The development of accurate real-time mechanical models of soft material deformation remains an active research area [2] [10] [3].

B. Haptic display device

The optimal display device would display any force or shape distribution to a user's finger tip regardless of the finger's position within a large workspace. Building a single device that meets this requirement is highly improbable at present, so a more practical approach is to divide the functionality between two devices: a "tactile display" that delivers distributed tactile sensation to the finger tip, which is mounted on an "arm" that delivers kinesthetic sensations across a large workspace (Fig. 3). Arms include traditional robot manipulators and force feedback devices.

For the purposes of the present discussion, tactile displays and arms may be roughly categorized by their mechanical impedance. High-impedance arms have high intrinsic stiffness at the tip of the arm, usually as a result of a high gear ratio (e.g. HapticMASTER, FCS Control Systems B.V., Schiphol, The Netherlands). Position control is straightforward but an external force sensor is required to render lower stiffness. Low-impedance arms (e.g. Phantom, Sensable Technologies, Woburn, MA, USA) are backdrivable and readily enable force control, but rendering high stiffness may require powerful motors and high resolution position sensing. A similar analysis applies to tactile display devices, see [11] for a review. Tactile shape displays (high-impedance) enforce a shape on the finger pad, usually through an array of mechanically actuated pins. Shape displays developed to date have reasonable performance (position resolution, pin spacing) at lower temporal bandwidths, typically a few dozen Hz. Tactile pressure displays (low-impedance) provide a force distribution against the finger pad. The few examples of this modality that have
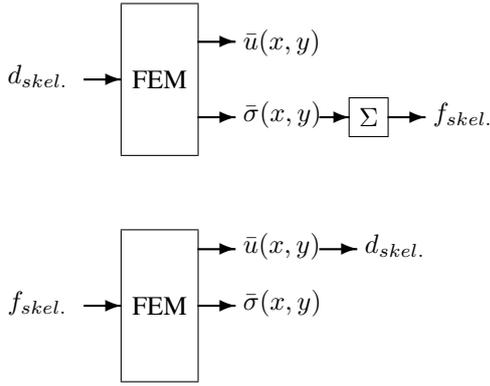
Fig. 2.   Finite element models.

Fig. 3.   Interaction between user and FEM

	Arm		Tactile Display	
Impedance	In	Out	In	Out
High Z	f	d	$\bar{u}$	$\bar{\sigma}$
Low Z	d	f	$\bar{\sigma}$	$\bar{u}$

been developed show good bandwidth but a limited force range.

In operation, the impedance of the devices determines the input and output parameters for the computational model for both kinesthetic and tactile feedback (Table I). For a low-impedance arm, the user imposes displacements d on the end of the arm. This sensed motion is relayed to the computational model, which calculates the appropriate kinesthetic force command f that the arm applies to the user's finger. For a high-impedance device, the user input is the force and the arm output is the displacement. A similar reasoning holds for tactile shape displays and tactile pressure displays.

A number of specialized approaches exist for stimulating specific forms of tactile feedback. Examples include simulating a homogeneous compliant material [12] and simulating a rigid lump under a fixed stiffness rubber [4]. While these approaches may offer high performance in a limited range of tactile stimulation, only pin-based tactile (shape or pressure) displays offer the possibility of displaying a wide range of tactile stimulation. We therefore focus our attention on pin style tactile displays.

Difficulties arise with certain pairings of kinesthetic and tactile display devices. For instance, pairing a shape display with a high-impedance arm would require a force sensor in between the positioner and the tactile display. Shape displays may be heavy, however, and will cause error in the force signal due to inertia and the dynamics of the display pins during operation.

In general, the choice of tactile display device impedance may not influence the configuration of the system. A complete mechanical model that calculates the full dynamic contact interaction will provide both the contact shape and contact pressure distribution across the finger as a function of either force or displacement input. If a simplified contact model is used, the model output must conform to the tactile display impedance. For example, a scaled surface deformation $\bar{u}(x,y)$ can provide the stress distribution output $\bar{\sigma}(x,Y)$ for a pressure display, or a scaled stress distribution can provide the surface deformation output for a shape display.
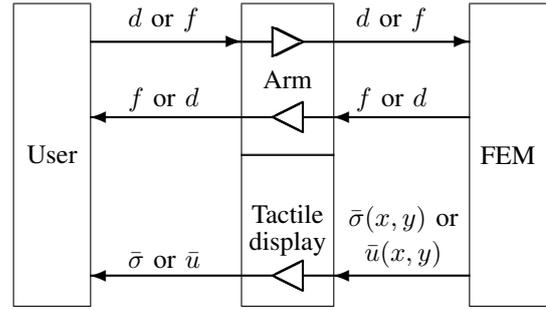
III. IMPLEMENTATION

We have shown that a number of design choices exist for constructing a large workspace compliance rendering system. For our implementation, we desired a research platform system with high performance and reliability with little consideration for size of apparatus. We chose a high-impedance pin-based shape display for the tactile display component because of its robustness and reasonable bandwidth. However, the drawback of a pin-based display is its weighty apparatus. Using a high-impedance positioning arm would require a force sensor in series with the large mass of the tactile display, resulting in a noisy force signal and/or damage to the force sensor. Therefore, we used a low-impedance, large workspace arm eliminating the need for a force sensor (Fig. 4). For the rendering program, we used a real time finite element modeling package allowing both haptic interaction and 3D visualization of a compliant object.

The tactile display is an array of mechanical pins actuated by commercially available radio controlled (RC) servomotors. The pins have diameters of 1 mm and an inter-pin spacing of 2 mm (Fig. 5). They have a maximum
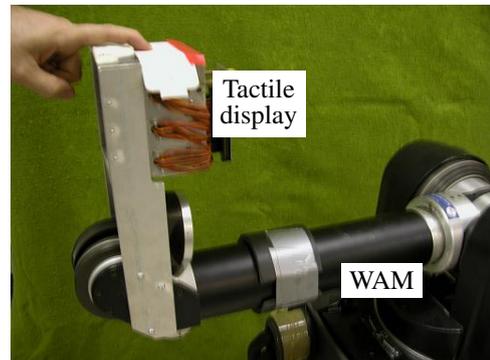

Fig. 4.   Entire system

Fig. 5. Tactile display pins

displacement of 2 mm and a vertical resolution of 0.1 mm. A 2 mm thick piece of silicone rubber (HSII RTV, Dow Corning) was placed on the pins of the tactile display as a spatial low-pass filter [13]. The tactile display can run at up to 25 Hz for small pin movements and 7.5 Hz for the full 2 mm pin displacement. The mass of the display apparatus is 1 kg. For a detailed device characterization on the shape display, please see [14].

A commercial low-impedance, large workspace robot arm is used as the kinesthetic force feedback device (Whole-Arm Manipulator (WAM), Barrett Technology, Cambridge, MA). The WAM was controlled using a 5000 Hz servo loop running on a digital signal processor (DS1103 PPC, dSPACE, Novi, MI). The tactile display was rigidly attached to the end of the first link of the robot arm, removing the wrist and distal link. Because the performance of the system depends on an accurate reproduction of force by the WAM, we used a feed-forward model of the forces on the arm. This feed-forward model consisted of torque ripple compensation, gravity compensation and friction compensation. The model and parameter fitting techniques are similar to the process used in [15]. Inertia is small since low accelerations are used during exploration. An inertia compensator is unnecessary because the effect of inertia compared to other feed-forward terms is also small.

A real-time finite element modeling package was used to determine the mechanical interactions between the finger and the rendered compliant material [3]. The modeler uses a tetrahedral discretization of the object domain to compute local deformations. To decrease computation time, an assumption is made that the stiffnesses of each node of the mesh, with respect to external displacements and forces, are linear. The FEM can be used to quickly determine the deformation $\bar{u}(x, y)$ of a compliant material in response to a force profile $\bar{\sigma}(x, Y)$, or determine the distributed contact force profile $\bar{\sigma}(x, Y)$ that results from an imposed position constraint $\bar{u}(x, y)$. This package provides support for visualization as well as haptic interaction. The finite element modeler ran on a separate workstation for a speed increase over the robot control computer and communicated with the robot control computer over Ethernet.

Our initial use of the system was to develop a one dimensional compliance renderer. Only the shoulder joint of the WAM was used to impart vertical forces and displacements,

while the base and roll joints were locked using a PID loop. The system accepts a user imposed motion, then calculates and displays both the kinesthetic forces and finger pad deformation that are felt when touching a compliant object. We used an 10,000 node, anisotropic tetrahedral mesh to simulate a compliant material 100 mm x 100 mm x 50 mm in size, with a Young's modulus of 2.5 kPa. The non-linear mesh distribution ensured a mesh resolution finer than the pin resolution of the tactile display in the area of exploration. Results could be precomputed and used in a lookup table to increase bandwidth of the system, along with disabling the graphical rendering of the mesh.

We used a parabolic pressure distribution based on previous characterizations of the mechanical properties of the finger pad [8] to approximate the finger-induced force applied on the surface of the mesh:

$$\forall X \backslash \left\{ \|X - X_0\| \leq \frac{d_0}{2} \right\},$$

$$p(X) = P_{max} - \frac{4 P_{max} \|X - X_0\|^2}{d_0{}^2} \qquad (1)$$

d_0 defines the diameter of the finger, X_0 the center of pressure and P_{max} the maximum pressure applied on the material. Thus, the external force applied on each vertex i of the mesh is:

$$F_i = \sum_{T \in C_i} \int_T \frac{p(X) ds}{3} \qquad (2)$$

where $T \in C_i$ defines the set of triangles T connected to vertex i. The corresponding mesh deformation was used to compute the net displacement d_{skel} and the surface deformation $\bar{u}(x, Y)$. The results were arranged in a lookup table to provide for the requirements of our low-impedance arm and high-impedance tactile display (d_{skel} input, f_{skel} and $\bar{u}(x, Y)$ output).

A. Arm characterization

To quantify the stiffness reproduction ability of the WAM, a force sensor (Gamma, ATI Industrial Automation, Apex, NC, force resolution = 0.05 N) was rigidly attached to the top of the tactile display. Position information was derived from the high resolution encoders of the WAM arm. Four stiffnesses were simulated (0.25 N/mm, 0.33 N/mm, 0.5 N/mm, 1.0 N/mm) and position and force information were recorded for a negative vertical displacement followed by a positive vertical displacement (Fig.6). Lines were fit to each dataset to find the closest stiffness. On average, the system displayed a stiffness with less than 17% error. Hysterises is also evident from the data, with an average histerisis of +/- 1.12 N.

To characterize the bandwidth of the system, the update rate of the renderer computing the mesh was measured under various conditions. The results are listed in Table II. Note that the bandwidths are dependent on the computer system used for computation, including the graphics card (Pentium 4, 1.8 GHz, 512 MB RAM). Network latency between the FEM computer and the robot control computer
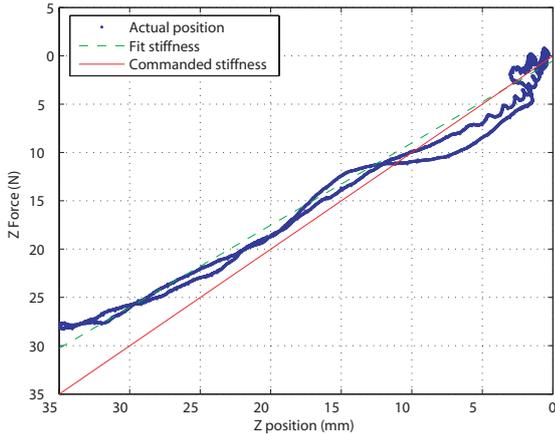
Fig. 6.   Actual rendered stiffness at 1.0 N/mm

TABLE II

FEM UPDATE RATES

FEM type	Visualization?	Update rate
Real time	Yes	5 Hz
Precomputed	Yes	20 Hz
Precomputed	No	1600 Hz

Fig. 7.   User stiffness discrimination ability

was measured to be less than 0.2 ms, so the update rate of the renderer was the limiting factor in system bandwidth.

IV. USER STUDY

Previous studies using real objects have shown that a person's compliance discrimination ability is more accurate when distributed tactile information is presented to the finger pad [16]. We attempt to duplicate this result to demonstrate the integration of the tactile and kinesthetic force feedback of our system.

In our study, users carried out a set of 80 forced choice trials where each trial consisted of two rendered material stiffnesses. Users palpated at their own rate and notified the experimenter when ready to feel the next material (approx. 2-5 seconds), then reported which material felt softer. One of the material stiffnesses was always 1.75 kPa. The comparison stiffnesses (1.875, 2.0, 2.25, 2.75, 3.75 kPa) were chosen by pilot studies to span the range of difficulty, from easy to distinguish to difficult to distinguish. Stiffness order (if the softer material was presented first or second) and comparison stiffness was counterbalanced across trials, with each user receiving the same trial order. Half the trials used both the shape display and the arm, the other half rendered the material using only the arm with the shape display pins locked at their maximum displacement. Use of the tactile display was alternated each trial so learning and fatigue effects were approximately equal for both conditions.

A force threshold of 2.5 N was used to limit the user's applied force to an input range where the linear assumption of the finite element model was still valid. If the user attempted to apply a force past the threshold, only the the threshold force would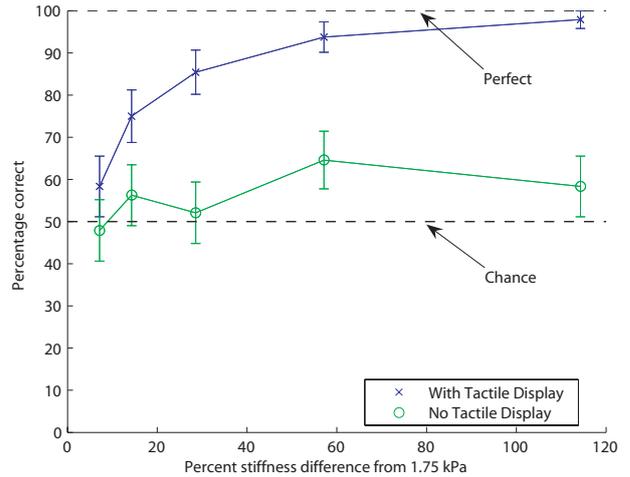 be displayed by the arm, giving no additional stiffness information. Similarly, the shape display would maintain the shape at the force threshold if the threshold was exceeded. Users were trained to apply forces less than the threshold.

A total of six graduate and undergraduate students, ages 21-27 years, volunteered for the study. All subjects defined themselves as right-handed and had no known abnormalities in either hand.

A. Results

Users were able to correctly discriminate stiffnesses in the presented range an average of 82% of the time with the tactile display and only 56% of the time without. Users demonstrated a consistent ability to correctly discriminate stiffness across the range of stiffnesses presented at a higher rate when using the tactile display (Figure 7). Without the tactile display, users did not perform statistically significantly different from chance ($t(239) = 1.28, p > 0.20$, two-tailed). From these results we conclude that the system is successful at displaying compliances and that the tactile display is a useful component in rendering a compliant material.

V. DISCUSSION

We have considered a number of design issues in generating a system that can render both the tactile and kinesthetic force feedback from a compliant environment. Tactile displays and robot arms can be classified by their impedance and that classification is useful in determining the structure of the system and the computational model. This design knowledge has been applied to the construction of a compliance rendering system, which integrates a tactile shape display, a low-impedance robot arm, a real time finite element modeler, and a 3D display. The system has been shown to effectively render compliance, both through device characterization and a user study. The study confirms the hypothesis that tactile force feedback is an important component in compliant environment rendering.

When using a force control device (low-impedance robot arm), the system performance is dependent on the open loop performance of our robot model. Because of hysteresis in our stiffness characterizations and errors in the rendered stiffness we conclude that unaccounted for forces are applied to the user. For instance, our friction model is limited by design and the accuracy of velocity estimates.

Bandwidth is another design issue. When users exceed the bandwidth of the system, there is a mismatch between devices. One example is the tactile display pins will fall quickly for a fast commanded motion. Bandwidth is also dependent on the update rate of the FEM software. Issues that affect FEM update rate are: visualization, precomputation, complexity of mesh/environment, complexity of interaction (solving contact problem, compliant model of the finger pad), assumptions (linearity), and simulated material properties (*i.e.* viscoelasticity). Computation hardware also affects the FEM update rate; a continued increase in computation power will result in an increase in simulation fidelity.

A number of design issues remain unaddressed for a complete virtual environment touch renderer. One difficulty is rendering both free motion and surface contact. Some simple solutions can be proposed, such as tracking the motion of the finger, maintaining contact with the device using a sleeve, or the user grabbing a handle. Each of these solutions has trade-offs with realism and safety. A more immersive approach has been described by Yokohiji, Hollis, Kanade [17] that involves tracking the motion of the hand and overlaying a visual display so that the user perceives the virtual environment with no disparity or offset between the visual and haptic feedback. The primary difficulty of this type of approach is sensing the imminent contact point between the user and the environment and having the device in place before contact is made.

VI. Acknowledgments

References

[1] S. Lederman and R. Klatzky, "Sensing and displaying spatially distributed fingertip forces in haptic interfaces for teleoperator and virtual environment systems," *Presence*, vol. 8, no. 1, pp. 86–103, 1999.

[2] C. Basdogan, S. De, J. Kim, M. Muniyandi, and M. Kim, H. amd Srinivasan, "Haptics in minimally invasive surgical simulation and training," *IEEE Computer Graphics and Applications*, vol. 24, no. 2, pp. 56–64, 2004.

[3] G. Picinbono, J. Lombardo, H. Delingette, and N. Ayache, "Improving realism of a surgery simulator: linear anisotropic elasticity, complex interactions and force extrapolation," *Journal of Visualization and Computer Animation*, vol. 13, no. 3, pp. 147–167, 2002.

[4] H. Iwata, H. Yano, and R. Kawamura, "Array force display for hardness distribution," in *Proceedings 10th Symposium on Haptic Interfaces for Virtual Environment and Teleoperator Systems*. Los Alamitos, CA, USA: IEEE Comput. Soc, 2002, pp. 165–171.

[5] W. Peine, "Remote palpation instruments for minimally invasive surgery," Ph.D. dissertation, Harvard University, 1998.

[6] P. Wellman, W. Peine, G. Favalora, and R. D. Howe, "Mechanical design and control of a high-bandwidth shape memory alloy tactile display," in *Experimental Robotics V. The Fifth International Symposium*, vol. 232. Barcelona, Spain: Springer-Verlag, 1994, pp. 56–66.

[7] D. Pawluk, W. Peine, P. Wellman, and R. Howe, "Simulating soft tissue with a tactile shape display," *ASME International Mechanical Engineering Congress and Exposition*, vol. 36, pp. 253–254, 1997.

[8] D. Pawluk and R. Howe, "Dynamic lumped element response of the human fingerpad," *ASME Journal of Biomechanical Engineering*, vol. 121, no. 2, pp. 178–184, 1999.

[9] ——, "Dynamic contact of the human fingerpad against a flat surface," *ASME Journal of Biomechanical Engineering*, vol. 121, no. 2, pp. 605–611, 1999.

[10] M. C. Cavusoglu, D. Feygin, and F. Tendick, "A critical study of the mechanical and electrical properties of the phantom haptic interface and improvements for high performance control," *Presence: Teleoperators and Virtual Environments*, vol. 11, no. 6, pp. pp. 555 – 568, 2002.

[11] M. Jungmann and H. Schlaak, "Miniaturised electrostatic tactile display with high structural compliance," in *Proceedings of the conference EuroHaptics 2002*, Edinburgh, U.K., 2002.

[12] G. Ambrosi, A. Bicchi, D. DeRossi, and E. Scilingo, "The role of contact area spread rate in haptic discrimintation of softness," in *Proceedings of the 1999 IEEE International Conference on Robotics and Automation*. Detroit, MI, USA San Diego, CA, USA: IEEE Comput. Soc. Press, 1999, pp. 305–10.

[13] J. M. Lee, C. R. Wagner, S. J. Lederman, and R. D. Howe, "Spatial low pass filters for pin actuated tactile displays," in *11th Annual International Symposium on Haptic Interfaces for Virtual Environment and Teleoperator Systems*, IEEE, Ed. Los Angeles, CA: IEEE, 2003.

[14] C. R. Wagner, S. J. Lederman, and R. D. Howe, "Design and performance of a tactile shape display using rc servomotors," *Haptics-e*, 2003.

[15] J. Desai and R. Howe, "Towards the development of a humanoid arm by minimizing interaction forces through minimum impedance control," in *Proceedings of the IEEE International Conference on Robotics & Automation*, Seoul, Korea, 2001.

[16] M. A. Srinivasan and R. H. LaMotte, "Tactual discrimination of softness," *Journal of Neurophysiology*, vol. 73, no. 1, pp. 88–101, 1995.

[17] Y. Yokokohiji, R. Hollis, and T. Kanade, "Wysiwyf display: A visual/haptic interface to virtual environment," *Presence*, vol. 8, no. 4, pp. 412–434, 1999.